Title
EVIDENCE FOR AN I = 3/2 BARTON RESONANCE AT 2020 MeV/c2

Authors
Chinowsky, W.
Condon, P.
Kinsey, R.R.
et al.

Publication Date
1967-08-01

UCRL-17651
cy. 2

University of California

Ernest O. Lawrence Radiation Laboratory

EVIDENCE FOR AN I = 3/2 BARYON RESONANCE AT 2020 MeV/c^2

W. Chinowsky, P. Condon, R. R. Kinsey, S. Klein,
M. Mandelkern, P. Schmidt, J. Schultz,
F. Martin, M. L. Perl, and T. H. Tan

August 1967

DISCLAIMER

UNIVERSITY OF CALIFORNIA

Lawrence Radiation Laboratory
Berkeley, California

August 23, 1967

ERRATA

TO: All recipients of UCRL-17651

From: Technical Information Division

Subject: UCRL-17651, "Evidence for an I = 3/2 Baryon Resonance at 2020 MeV/c^2" by W. Chinowsky, P. Condon, R. R. Kinsey, S. Klein, M. Mandelkern, P. Schmidt, J. Schultz, F. Martin, M. L. Perl, and T. H. Tan, August 1967.

Please make the following corrections on subject report.

Title page, first line should read "Submitted to Physical Review Letters".

Page 1, last sentence, first paragraph. Delete hyphen to change "strange-particle" to "strange particle."

Page 5, third line from the bottom. Delete superscript on "Λ" so it now reads "$\Lambda K^+ \pi^+$."

Page 6, 12th line. Change 2060 to 2160.

Page 7, line 16. Delete superscript on "Λ" to read "decay $N^*(2020) \to \Lambda K^+ \pi^+$."

Page 8, line 12. Change $M(n\pi^+)$ to read $M(\Lambda\pi^+)$.

Page 9, line 7. Change 2060 to 2160.
line 10. Correct punctuation from "region, are as before," to "region are, as before, ..."
line 18. Change 1924 to 1920.

Page 11, References

a) Order of names in Reference 1 should be changed so that F. Martin follows J. Schultz.

b) Reference 2 should read:

2. E. Pickup, D. K. Robinson, and E. O. Salent, Phys. Rev. 125, 2091 (1962).

c) Reference 3 should read:

3. E. L. Hart, R. I. Louttit, D. Luers, T. W. Morris, W. J. Willis, and S. S. Yamamoto, Phys. Rev. 126, 747 (1962).

Submitted to Physics Review Letters

UCRL-17651
Preprint

UNIVERSITY OF CALIFORNIA

Lawrence Radiation Laboratory
Berkeley, California

AEC Contract No. W-7405-eng-48

EVIDENCE FOR AN I = 3/2 BARYON RESONANCE AT 2020 MeV/c^2

W. Chinowsky, P. Condon, R. R. Kinsey, S. Klein,
M. Mandelkern, P. Schmidt, J. Schultz,
F. Martin, M. L. Perl, and T. H. Tan

August 1967

EVIDENCE FOR AN I = 3/2 BARYON RESONANCE AT 2020 MeV/c^2 *

W. Chinowsky, P. Condon†, R. R. Kinsey, S. Klein, M. Mandelkern, P. Schmidt and J. Schultz†

Physics Department and Lawrence Radiation Laboratory, University of California, Berkeley, California

and

F. Martin, M. L. Perl, and T. H. Tan

Stanford Linear Accelerator Center, Stanford, California

The existence of every presently known zero-strangeness baryon resonance has been established through its coupling to the pion nucleon system. However, the possibility that there are baryon resonances which are only weakly coupled to this channel is not excluded. A study of proton-proton interactions at 6 GeV/c has resulted in the evidence presented here for such a resonance with isotopic spin 3/2, mass 2020 ± 30 MeV/c^2 and width 225 ± 50 MeV/c^2. The dominant decay modes observed are $N^*(1236)\pi\pi$, $N^*(1236)\rho$ and the strange-particle final state $Y^*(1385)K$.

The enhancements observed in this experiment which lead to the conclusion of a new resonance are in the mass region 2040 to 2080 MeV/c^2. Because of the proximity of this resonance to threshold for the dominant decay modes, it is probable that the observed peaks are significantly shifted from the central resonance mass. Lack of reliable information on the spin-parity, and hence on angular momentum configurations of

* Work performed under the auspices of the U. S. Atomic Energy Commission.

† Present address: University of California, Irvine.

Subject category 63.6

the decays, prevents us from performing a definitive determination of the central mass value. A preliminary fit described in Section B yields the value 2020 MeV/c^2 quoted above.

Details of the experimental arrangement used to obtain approximately 550,000 pictures of interactions of incident protons of 6.04 ± 0.03 GeV/c in the LRL 72-inch liquid hydrogen bubble chamber are discussed more fully elsewhere.[1] All photographs were scanned for strange-particle production events, but only a sample, some 112,000 pictures, were scanned for nonstrange events, that is, events without visible charged or neutral decays. The latter were measured on the LRL flying spot digitizer. The three-view geometric reconstruction program FOG was used to reconstruct the events and fitting with the kinematical constraints was done by the program CLOUDY. Events with visible charged or neutral strange particle decays were measured on more conventional "Vanguard" and "Franckenstein" digitizing machines. These events were processed through the geometric reconstruction and kinematic fitting program PACKAGE. The analysis of the two types of events will be discussed separately.

A. Nonstrange Particle Events

Approximately 33,000 nonstrange four-prong events were measured by the FSD. The identified final states and their cross sections are

(1) $p\,p \rightarrow p\,p\,\pi^+\,\pi^-$ 3.2 ± 0.3 mb

(2) $p\,p \rightarrow p\,n\,\pi^+\,\pi^+\,\pi^-$ 3.1 ± 0.5 mb

(3) $p\,p \rightarrow p\,p\,\pi^+\,\pi^-\,\pi^0$ 2.4 ± 0.4 mb

Reaction (1) is dominated by peripheral production of pseudo-two-body final states NN^* and N^*N^*. This observation is consistent with results of earlier work[2-4], as is the lack of ρ-meson production in the four body state. Reactions (2) and (3), however, yield particles whose final state interactions are qualitatively different. In particular, analysis of events identified as examples of process (2) has revealed evidence for ρ-meson production with the $\pi^+\pi^-$ mass spectrum showing a peak in excellent agreement with the known ρ properties. In addition a strong correlation is observed among the particles $p\pi^+\pi^+\pi^-$. Figs. 1(a) and (b) show the mass spectra of the four body system and the two pion system respectively. The observed enhancement in the effective mass distribution of the four particle system is particularly strong in the restricted sample of events for which the requirement is made that the $n\pi^-$ mass be outside the range 1220 ± 100 MeV/c^2, as shown in the first histogram of Fig. 1(a). Comparison of the experimental $p\pi^+\pi^+\pi^-$ effective mass distribution with the superimposed phase space distribution shows a peak near 2080 MeV/c^2 with a width of about 200 MeV/c^2. We point out that the phase space distribution is shown for purposes of illustration and this particular shape or normalization of smooth background is not necessary for the argument. Indeed, various background distributions, including effects of numerous known resonances among the final state particles, are all similar in shape. The height of the peak, that is, the number of events above background assigned to the N^*(2020) resonance is essentially unaltered when such differently generated backgrounds are considered. The particular curve shown is the result of a Monte Carlo generation of a phase space background with the $n\pi^-$ effective mass cut and the assumption that the final state consists of 64 percent $np\pi^+\pi^+\pi^-$ and 36 percent $nN^{*++}(1236)\pi^+\pi^-$, as suggested by the $p\pi^+$ mass spectrum. Observation of the $N^*(2020)$ in this state, with $I_Z = 3/2$, establishes the isotopic spin of the resonance, $I = 3/2$.

A similar peak at this mass is observed in the $p\pi^+\pi^-\pi^0$ effective mass distribution of reaction (3). However, we present the characteristics of the final state $np\pi^+\pi^+\pi^-$ in greater detail since it has proved possible to eliminate background events with confidence and also because the production cross sections of interest are largest here. The second histogram of Fig. 1(a) and the unshaded histogram of Fig 1(b) show the effect of requiring that at least one $p\pi^+$ combination have an effective mass in the range 1220 ± 60 MeV/c^2, in addition to the cut on the $n\pi^-$ effective mass. If both π^+ mesons of reaction (2) meet this requirement then both $\pi^+\pi^-$ effective mass combinations are included in Fig. 1(b). In fact in only 259 of 1492 events were both $p\pi^+$ effective masses within the limits. Including both combinations in the histograms does not affect the ρ peak but only increases the smoothly varying background. We note that in the second histogram of the $N^{*++}(p\pi^+)\pi^+\pi^-$ effective mass in Fig. 1(a) the number of background events has been reduced but that the number of events in the $N^*(2020)$ peak has not changed significantly, indicating that the $N^*(1236)$ is a very important intermediate decay product and may be present in all decays of the $N^*(2020)$ into the nucleon-three pion system.

The third histogram in Fig. 1(a) and the shaded histogram of

Fig. 1(b) show the effect of the additional requirement $|\cos\theta_n| \geq 0.9$, where θ_n is the angle between the neutron and the incident proton direction in the total center of mass system. Again no significant change is noted in the $N^*(2020)$ peak of the $N^{*++}(p\pi^+)\pi^+\pi^-$ effective mass distribution indicating the peripheral character of the $N^*(2020)$ production.

To estimate the branching ratio of $N^*(2020)$ decay into $N^*(1236)\rho$, a selection of events was made where, in addition to the limits described above on the $p\pi^+$ and $n\pi^-$ effective masses and the center of mass angle of the neutron, we require the $\pi^+\pi^-$ effective mass to be in the range 740 ± 100 MeV/c^2. Except for five events, this selection uniquely assigns the π^+'s to either the N^* or the ρ. The $N^{*++}(p\pi^+)\rho(\pi^+\pi^-)$ effective mass distribution of these events is shown in Fig. 2(a). The $N^*(2020)$ is clearly present and from the magnitude of the peaks we estimate the branching ratio $N^{*++}(2020) \rightarrow N^{*++}(1236)\rho/N^{*++}(2020) \rightarrow$ all $p\pi^+\pi^+\pi^-$ final states $= 0.6 \pm 0.1$. This result is somewhat obscured by the presence of $N^*(1920)$ indicated in the $p\pi^+\pi^+\pi^-$ mass spectra. Separating this peak from the $N^*(2020)$ is difficult with the present data. For this reason also we have not attempted to determine the resonance parameters by fitting the experimental distributions in $p\pi^+\pi^+\pi^-$ mass with some theoretical model. A much cleaner $N^*(2020)$ peak is observed in the strange particle decay mode. The mass and width determined from the $\Lambda^oK^+\pi^+$ distribution discussed below are more reliable estimates than can be determined from the nonstrange data. The $p\pi^+\pi^+\pi^-$ mass distribution is quite consistent with that expected to result from production of $N^*(2020)$ with those characteristics together with a contribution from $N^*(1920)$ and a phase space background. We also note some enhancement in the 2400 MeV/c^2 region which could be associated with the $I = 3/2$ $N^*(2420)$ but since the effective mass distribution of the possible background final states all peak in this region no conclusion can be made concerning the production of this resonance.

That the $N^*(2020)$ is a resonance and not, perhaps, a kinematic enhancement is supported by the decay angular distributions of Figs. 3(a) and (b). Fig. 3(a) shows the angular distribution of the $N^*(1236)$ in the $N^*(1236)\rho$ center of mass for those events in the resonance region defined as $1960 \leq M(N^*\rho) \leq 2060$ MeV/c^2. This distribution is consistent with symmetrical forward-backward peaking while the nonresonant events shown in Fig. 3(b) have only a forward peak. The incident proton used to define the reference direction for these angular distributions is selected as that proton which yields the smaller absolute value of momentum transfer to the $N^*\rho$ system, consistent with the observed peripheral character of the production process.

Similar selections to isolate other possible decay modes resulting from reactions (2) and (3) produce samples of events more confused by background and in addition contain only $I_Z = 1/2$ states of the $N^*(2020)$. Consideration of isotopic spin conservation then leads us to expect smaller cross sections. Indeed the isotopic spin assignment is supported by the fact that the $I_Z = 1/2$ channels all have rather small cross sections. The estimated cross sections for $N^*(2020)$ production and subsequent decay into the final states investigated are

$pp \rightarrow nN^{*++}(2020)$, $N^{*++}(2020) \rightarrow p\pi^{+}\pi^{+}\pi^{-}$		65 ± 16 μb
$pp \rightarrow pN^{*+}(2020)$, $N^{*+}(2020)$	$\rightarrow n\pi^{+}\pi^{+}\pi^{-}$	< 6 μb with 90% confidence level
$pp \rightarrow pN^{*+}(2020)$, $N^{*+}(2020)$	$\rightarrow p\pi^{+}\pi^{-}\pi^{0}$	20 ± 6 μb.

B. Strange Particle Events

The strange particle reactions which have been studied and their production cross sections are:

(4)	$pp \rightarrow \Lambda pK^{0}\pi^{+}$	67 ± 10 μb
(5)	$pp \rightarrow \Lambda pK^{+}\pi^{0}$	45 ± 7 μb
(6)	$pp \rightarrow \Lambda nK^{+}\pi^{+}$	50 ± 7 μb

An enhancement at about 2040 MeV/c^2 has been observed in the $\Lambda K\pi$ mass spectra for each of these reactions. The $\Lambda K^{+}\pi^{+}$ mass distribution for reaction (6) is shown as the unshaded histogram of Fig. 1(c). For comparison, we have included a background curve which is calculated as a mixture of 82 percent non-resonant phase space and 18 percent $nY^{*}K$ resonant background. We attribute this enhancement to the alternate decay $N^{*}(2020) \rightarrow \Lambda^{0}K^{+}\pi^{+}$. This final state again confirms the isotopic spin 3/2 assignment. This pure isotopic final state is the most useful strange particle final state for studying the properties of the resonance. In addition, there is no background from the $K^{*}(890)$ and essentially none from the $N^{*}(1236)$, which is not the case in the other two channels. From this point on, then, discussion will be restricted to the $\Lambda nK^{+}\pi^{+}$ channel.

To provide a pure sample, exploiting the peripheral production of the resonance, a selection of events was made requiring $|\cos\theta_n| \geq 0.9$, where as before θ_n is the angle between the neutron and the beam proton in the center-of-mass system. The $\Lambda K^+\pi^+$ mass spectrum for these events is plotted as the shaded area in Fig. 1(c). This selection clearly enhances the peak at 2040 MeV/c^2.

The $\Lambda\pi^+$ mass spectrum of Fig. 1(d) shows a peak of mass and width in excellent agreement with the known $Y^*(1385)$, and we estimate that 35 percent of the events in this channel are associated with Y^* production. The shaded area of Fig. 1(d) corresponds to the same neutron angle cut as above.

That the $N^*(2020)$ decay in this channel is almost entirely into $Y^{*+}K^+$ is clearly demonstrated in Fig. 2(b). Here we have plotted the $\Lambda K^+\pi^+$ mass spectrum with a selection on the $\Lambda\pi^+$ mass, $1350 \leq M(n\pi^+) \leq 1420$ MeV/c^2, and with the same requirement on the neutron angle as before. The number of events in the resonant peak remains the same after this selection. This distribution is evidently quite free of background and from it we have determined the resonance parameters $M_o = 2020 \pm 30$ MeV/c^2 and $\Gamma_o = 225 \pm 50$ MeV/c^2, using a maximum likelihood fit to this data. Since the angular momentum of the decay is not determined we have, for simplicity, fit the data with a simple $\ell = 0$ Breit-Wigner. The use of higher ℓ wave Breit-Wigner line shapes tends to shift the mass to lower values. As stated above, this fit also gives excellent agreement with the observed enhancement in the nonstrange data. Since the kinematic properties are quite different for the strange and nonstrange final states, this tends to exclude the possibility that the observed enhancements result from some accidental effect of kinematic origin and to support the conclusion of a genuine resonance.

For reaction (6) we also examine the decay angular distribution in the Y^*K rest frame. The angle is defined between the Y^* direction and that initial proton from which the Y^*K system has the smaller absolute value of momentum transfer. The distribution in Fig. 3(c) is for events with $1960 \leq M(\Lambda K^+\pi^+) \leq 2060$ MeV/c^2 and Fig. 3(d) for events not having $M(\Lambda K^+\pi^+)$ within these limits. In both cases $|\cos \theta_n| \geq 0.9$. The events with $M(\Lambda K^+\pi^+)$ values corresponding to the resonance region, are as before, consistent with backward-forward peaking which is characteristic of resonance production and decay.

The small number of events in our angular distributions precludes a determination of the spin and parity of the $N^*(2020)$. However, we can exclude a $J = 1/2$ assignment which would predict an isotropic distribution, contrary to what is observed. We may speculate, however, that the $N^*_{3/2}(2020)$ has $J^P = 7/2^-$. This would be the prediction based on a Regge pole model if the $N^*_{3/2}(2020)$ is the parity partner of the $N^*_{3/2}(1924)$.[5]

Other production reactions and possible decay modes of the $N^*(2020)$ are being investigated. No significant enhancement is seen in the Σ^+K^+ mass spectrum of the Σ^+K^+n final state.[1] Some slight enhancement is observed in the $\Lambda K\pi$ mass of the $\Lambda NK\pi\pi$ final states. Possible detection of this resonance in other nonstrange channels is obscured by background problems and competition with other baryon resonances. The $p\pi^+$ mass spectrum of the $p\pi^+n$ final state has been studied thoroughly. However, the $N^*(1920)$ dominates the high mass region and there is no obvious $N^*(2020)$ present. From our observation of the $Y^{*+}K^+$ decay of the $N^*(2020)$, we would expect that $N^*(1236)\pi$ would be a strong decay mode; indeed it may be the dominant one. However, the $I_z = 3/2$ decay of the $N^{*++}(2020)$ into $N^*(1236)\pi$ cannot be investigated in the $nN^{*++}(2020)$ final state since this would require the detection of two neutral particles.

An observation has been reported[6] of a much narrower enhancement at 2080 MeV/c^2 in the combined $N^*(1236)\rho$ system produced in π^-p collisions. This peak was observed in an $I_z = 1/2$ state and was resolved from another narrow peak at 2190 MeV/c^2. Whether that 40 MeV/c^2 wide peak is related to the broad peak reported here is an open question.

We acknowledge, with gratitude, the coöperation of Professor Luis Alvarez in making the bubble chamber available and Professor Emilio Segrè's much appreciated advice and support. Dedicated performance of the operating crews of the bevatron and bubble chamber and of the scanners and data analysis personnel were essential to the performance of the experiment and we thank them all.

REFERENCES

1. W. Chinowsky, R. R. Kinsey, S. L. Klein, M.A. Mandelkern, F. Martin, J. Schultz, M. L. Perl, and T. H. Tan, Production of K mesons in Three-Body States in Proton-Proton Interactions at 6 BeV/c, Phys. Rev. (to be published) (UCRL-17619).

2. D. V. Bugg, A. J. Oxley, J. A. Zoll, J. G. Roshbroke, V. E. Barnes, J. B. Kinson, W. P. Dodd, G. A. Doran, and L. Riddiford, Phys. Rev. 133, B1017 (1964).

3. A. M. Eisner, E. L. Hart, R.I. Louttit, and T. W. Morris, Phys. Rev. 138, B670 (1965).

4. G. Alexander, O. Benary, G. Czapek, B. Haber, N. Kidron, B. Reuter, A. Shapira, E. Simopoulou, and G. Yekutieli, Proton-Proton Interactions at 5.5 GeV/c, (to be published) (Nuclear Physics Department, Weizmann Institute of Science, Rehovoth, Aug. 1966).

5. G. Chew and C. Chiu, private communication.

6. T. S. Yoon, P. Berenzi, A. W. Key, J. D. Prentice, N. R. Steenberg, and W. D. Walker, Phys. Letters, 24B, 307 (1967).

FIGURE CAPTIONS

Fig. 1. (a) and (b) are the $p\pi^+\pi^+\pi^-$ and $\pi^+\pi^-$ mass spectra respectively for the $np\pi^+\pi^+\pi^-$ final state. The unshaded mass spectrum of (a) is for those events with $M(n\pi^-)$ outside the $N^*(1236)$ band (2521 events). The first shaded histogram of (a) and the unshaded histogram of (b) correspond to the additional requirement that $M(p\pi^+)$ be in the $N^*(1236)$ band. (1492 events, 1751 combinations in (b).) The second shaded histogram of (a) and the shaded histogram of (b) correspond to the added requirement that the absolute value of the cosine of the production angle of the neutron be greater than 0.9. (582 events, 704 combinations in (b).) (c) and (d) are the $\Lambda K^+\pi^+$ and $\Lambda\pi^+$ mass spectra respectively for the $n\Lambda K^+\pi^+$ final state. Unshaded histograms are for the total sample (680 events). The shaded histograms are for events with the absolute value of the cosine of the production angle of the neutron greater than 0.9 (225 events).

Fig. 2. (a) Mass spectrum of $N^{*++}(1236)\rho^0$ from the final state $nN^{*++}(p\pi^+)\rho^0(\pi^+\pi^-)$ (193 events) and (b) the $Y^{*+}(1385)\,K^+$ mass spectrum from the $nY^{*+}(\Lambda\pi^+)K^+$ final state (100 events) with the requirement in both cases that $|\cos\,\theta_n| \geq 0.9$.

Fig. 3. (a) and (b) Angular distribution of the $N^{*++}(1236)$ in the $N^{*++}(1236)\rho^0$ center of mass in the resonant region and outside the resonant region respectively. (c) and (d) angular distribution of the $Y^{*+}(1385)$ in the $Y^{*+}(1385)K^+$ center of mass in the resonant region and outside the resonant region respectively.

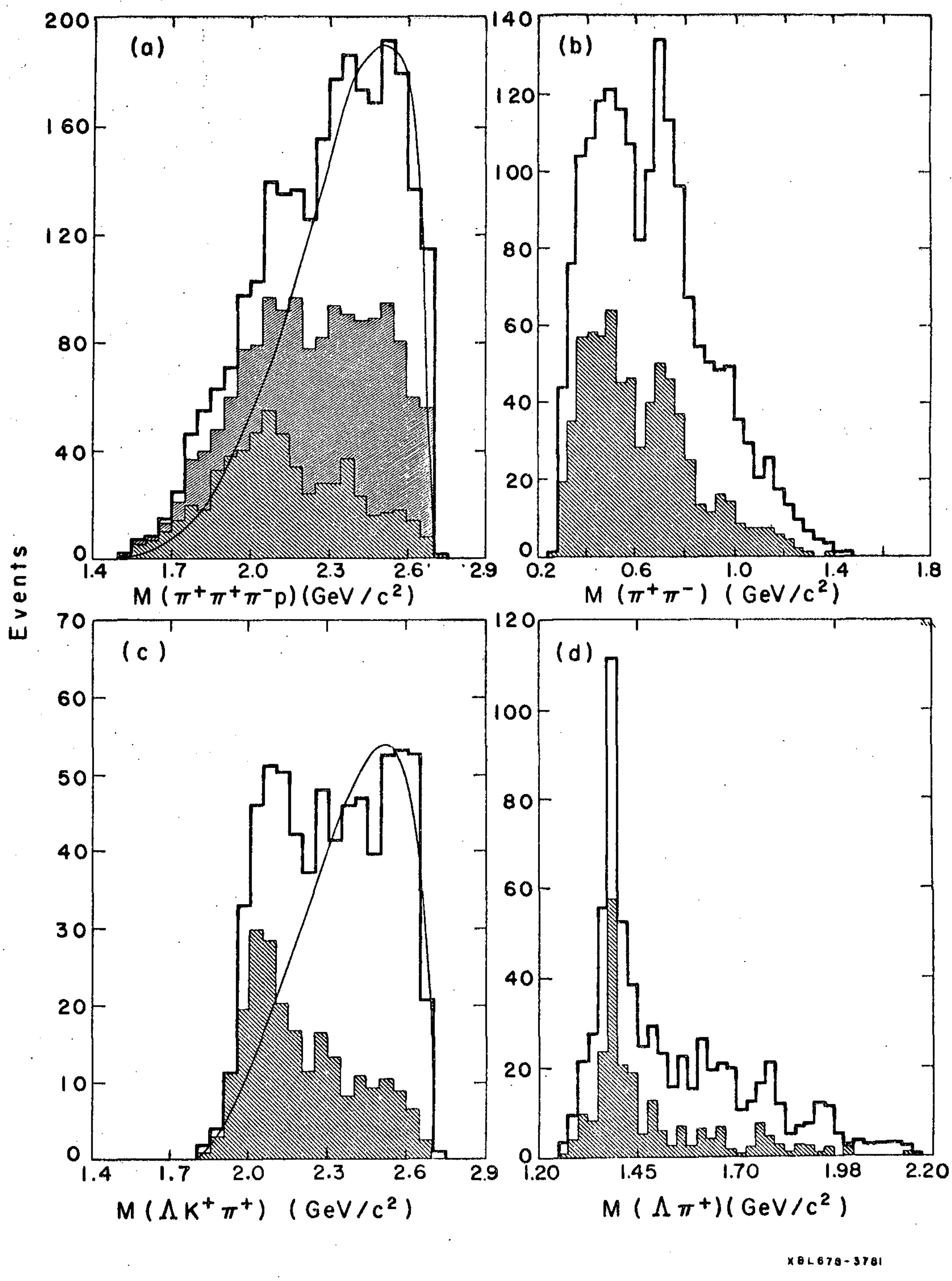

Events
(a)
(b)
(c)
(d)
M (π⁺π⁺π⁻p)(GeV/c²)
M (π⁺π⁻) (GeV/c²)
M (ΛK⁺π⁺) (GeV/c²)
M (Λπ⁺)(GeV/c²)
XBL 678-3781

Fig. 1

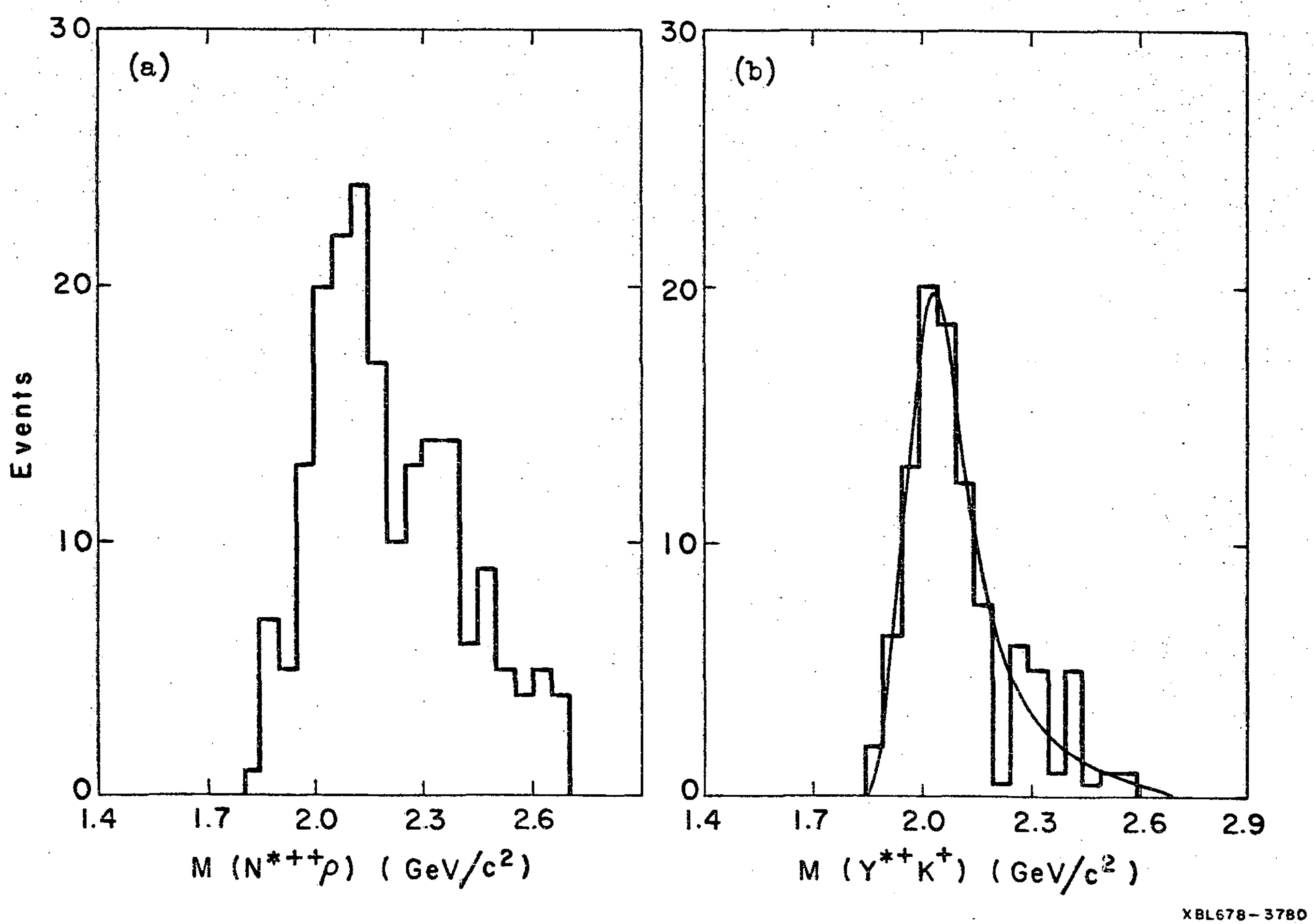
30
20
10
0
Events
(a)
1.4
1.7
2.0
2.3
2.6
M (N*++ρ) (GeV/c2)
(b)
2.9
M (Y*+K+) (GeV/c2)
XBL678-3780

Fig. 2

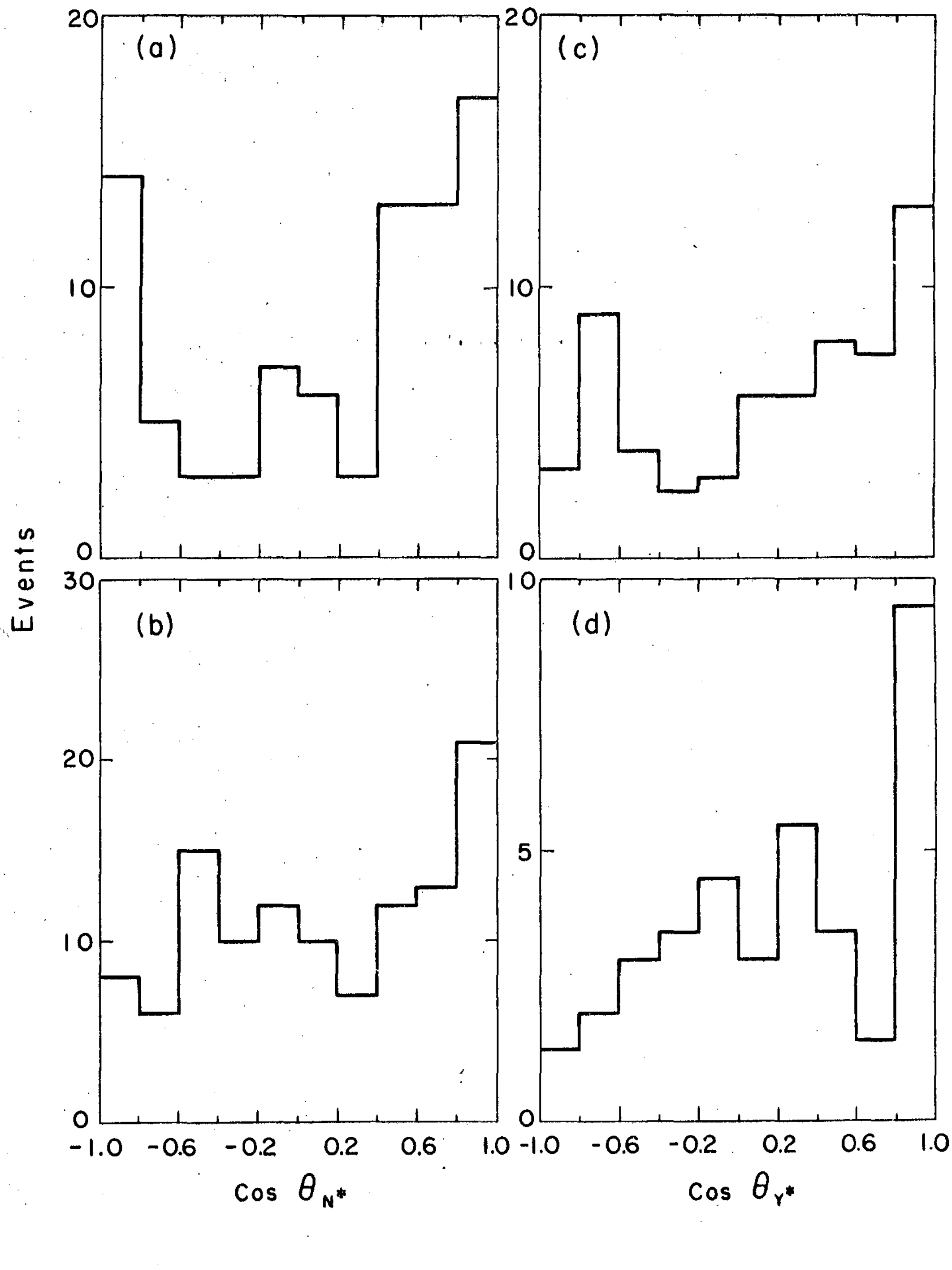
(a)
(b)
(c)
(d)
Events
20
10
0
30
20
10
0
20
10
0
10
5
0
-1.0
-0.6
-0.2
0.2
0.6
1.0
Cos θ_{N^*}
Cos θ_{Y^*}
XBL676-3782

Fig. 3